11.4 BUDGETS OF SCALAR FLUXES FOR CLOUDY BOUNDARY LAYERS

Rieke Heinze[1],* Dmitrii Mironov[2] and Siegfried Raasch[1]

[1] Institute of Meteorology and Climatology, Leibniz University Hannover, Germany
[2] German Weather Service, Offenbach am Main, Germany

1. INTRODUCTION

In numerical weather prediction and climate models, turbulence has to be parameterized because the scales of turbulence are much smaller than the grid spacing typically used. Most turbulence closure models are based on truncated ensemble-mean budget equations for the second-order moments of fluctuating velocity and scalar fields. Although these budgets have a fundamental importance for turbulence modeling, there is still a lack of systematic and comprehensive analysis of second-moment budgets, especially for cloudy boundary layers. There are numerous large-eddy simulation (LES) studies which focus on the turbulence kinetic energy (TKE) budget of cloudy boundary layers (e.g. Moeng, 1986; Brown, 1999; Chlond and Wolkau, 2000). However, other second-moment budgets, for example, budgets of scalar variances (e.g. de Roode and Bretherton, 2003; Neggers, 2009) and of Reynolds stress (e.g. Cuijpers et al., 1996), are poorly investigated. Using very high resolution LES of cumulus-topped and stratocumulus-topped boundary layer flows, we have performed a detailed analysis of the budgets of the Reynolds stress (including its trace, i.e. the TKE), of the scalar fluxes, and of the scalar variances. The present study focuses on the scalar-flux budgets. The main question addressed here is how the scalar-flux budgets and the so-called pressure-scrambling terms in the budgets behave in the presence of shallow clouds.

Modeling the pressure-scrambling terms, i.e. the pressure-scalar and pressure-velocity covariances in the scalar-flux and Reynolds-stress budgets, is one of the key issues in second-order turbulence modeling (e.g. Mironov, 2001, 2009; Hanjalić and Launder, 2011). Using data sets generated with LES, models (parameterizations) of the pressure-scrambling terms have been tested for dry convective (Moeng and Wyngaard, 1986; Mironov, 2001) and neutral (Andrén and Moeng, 1993) boundary layers. Similar tests for cloudy boundary layers were not performed so far. In the present study, some parameterizations of the pressure-scrambling terms in the scalar-flux budgets are tested against data from LES of cloudy boundary layers. Based on the conventional modeling approach for the pressure terms (e.g. Hanjalić and Launder, 2011), the pressure-scalar covariances are decomposed into contributions due to nonlinear turbulence-turbulence interactions, mean velocity shear, buoyancy, and Coriolis effects, and models (parameterizations) for these contributions are tested against LES data. It should be noted that such tests can only be performed on the basis of numerical data from LES or from direct numerical simulations. Apart from the fact that in situ measurements of fluctuating pressure are rather difficult (Wilczak and Bedard, 2004), the above decomposition of the fluctuating pressure is simply impossible on the basis of observational data.

In what follows, a standard notation is used where t is time, $x_i = (x,y,z)$ are the Cartesian coordinates, $u_i = (u,v,w)$ are the velocity components. θ is the potential temperature, θ_v is the virtual potential temperature, q_v is the water vapor specific humidity, p is the perturbation pressure, g is the acceleration due to gravity, f is the Coriolis parameter, and θ_0 and ρ_0 are reference values of potential temperature and density, respectively. A generic variable s denotes a quasi-conservative scalar, that is either the liquid water potential temperature θ_l or the total water specific humidity q. The Einstein summation convention for repeated indices is used. An overbar $\overline{()}$ and a single prime $()'$ denote a resolved-scale (filtered) variable carried by the LES model and a deviation therefrom (i.e. a sub-filter scale fluctuation), respectively. A horizontal mean is denoted by angle brackets $\langle() \rangle$, and a deviation therefrom (i.e. a fluctuation of the filtered quantity about a horizontal mean) is denoted by a double prime $()''$. Then, a fluctuating variable a can be represented as $a = \langle \overline{a} \rangle + \overline{a}'' + a'$.

2. LES MODEL AND SIMULATED CASES

In this study, the parallelized large-eddy simulation model PALM (Raasch and Schröter, 2001; Riechelmann et al., 2012) is applied. Using the finite difference technique, the model solves the filtered, non-hydrostatic Navier-Stokes equations in the Boussinesq approximation and the filtered transport equations

*Corresponding author address: Rieke Heinze, Institut für Meteorologie und Klimatologie, Leibniz Universität Hannover, Herrenhäuser Str. 2 D-30419 Hannover, Germany; e-mail: heinze@muk.uni-hannover.de

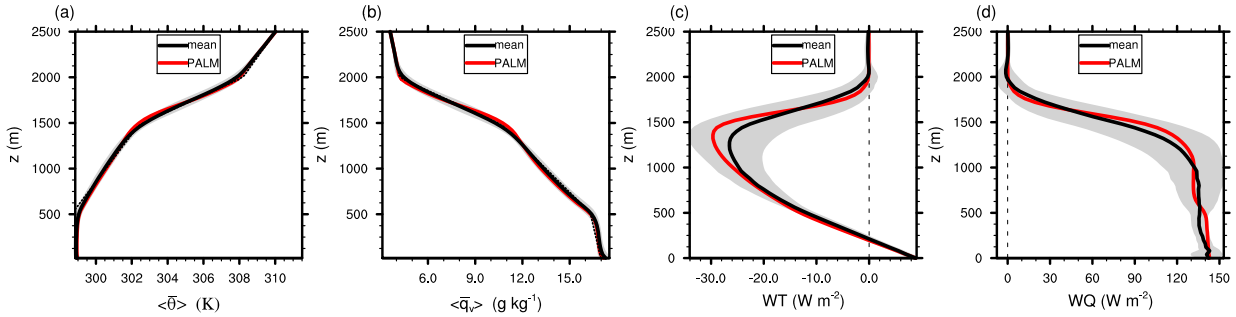

Figure 1: Vertical profiles of potential temperature $\overline{\theta}$ (a), specific humidity $\overline{q}_\mathrm{v}$ (b), vertical flux WT of the liquid water potential temperature (c), and vertical flux WQ of the total water specific humidity (d) for the BOMEX case. Black lines show profiles averaged over all models participating in the BOMEX LES intercomparison study, and the grey shading shows twice the standard deviation for the model ensemble (see Siebesma et al., 2003, for details). Red lines show the PALM output. Profiles of $\overline{\theta}$ and $\overline{q}_\mathrm{v}$ are obtained by means of averaging over one hour of simulations, and profiles of WT and WQ are the result of averaging over three hours.

for two quasi-conservative thermodynamic variables, viz., the liquid water potential temperature and the total water specific humidity. The filtering of the governing equations is carried out implicitly, following the volume-balance approach (Schumann, 1975). The incompressibility of the flow is ensured by solving a Poisson equation for the perturbation pressure, using a predictor-corrector method and a fast Fourier transform. The sub-grid scale (SGS) closure model is based on Deardorff (1980), where the SGS fluxes of momentum and scalars are determined through the down-gradient approximation and a prognostic equation for the SGS TKE is carried to determine the SGS eddy diffusivity. The resolved-scale liquid water content $\overline{q}_\mathrm{l}$ is calculated by means of a simple saturation adjustment scheme based on Cuijpers and Duynkerke (1993), where a grid volume is regarded as cloudy when the total water content is larger than the saturation specific humidity (all-or-nothing method that does not account for the fractional cloud cover at sub-grid scales). Advection of velocity and scalars is computed by a fifth-order scheme based on Wicker and Skamarock (2002). A third-order Runge-Kutta scheme with a variable time step is used for time advance.

The set-up of our simulations is based on two GEWEX Cloud System Study LES test cases. These are (i) the shallow trade-wind cumulus case BOMEX (Siebesma et al., 2003) and (ii) the nocturnal stratocumulus case DYCOMS-II (RF01) (Stevens et al., 2005). The major difference between our simulations and the BOMEX and DYCOMS simulations is in the grid spacing. As compared to a rather coarse standard resolution of BOMEX (with the mesh size of 100 m, 100 m and 40 m in x, y and z direction, respectively) and DYCOMS (mesh size of 100 m, 100 m and 40 m), a much finer resolution with a mesh size of 5 m in all directions is used in the present study. Furthermore, the horizontal domain size for the DYCOMS case is nearly doubled to become 6.4 km × 6.4 km which is the same as for the BOMEX case. Among other things, a larger domain yields improved estimates of turbulence moments computed on the basis of LES model output.

Vertical profiles of mean scalar fields and of the vertical scalar fluxes computed by PALM are compared with available LES data from the BOMEX and DYCOMS studies. In Figs. 1 and 2 (all figures are produced with NCL, 2012), $\mathrm{WT} = \left\langle \overline{w}''\overline{\theta}_\mathrm{l}'' \right\rangle + \langle \tau_{\theta 3} \rangle$ and $\mathrm{WQ} = \langle \overline{w}''\overline{q}'' \rangle + \left\langle \tau_{\mathrm{q}3} \right\rangle$ represent total (i.e. resolved + sub-grid) vertical scalar fluxes. The SGS fluxes of liquid water potential temperature and total water specific humidity, $\tau_{\theta 3}$ and $\tau_{\mathrm{q}3}$, respectively, are computed by the SGS model. A three-layer structure of the BOMEX boundary layer with a well-mixed subcloud layer at $z < 500\,\mathrm{m}$, a conditional unstable layer at $500\,\mathrm{m} \leq z \leq 1500\,\mathrm{m}$ and an inversion at $z > 1500\,\mathrm{m}$ is clearly seen in Figs. 1a and 1b. The profiles of WT and WQ computed by PALM are very close to the ensemble-mean profiles from the BOMEX study, see Figs. 1c and 1d. The PALM profiles plotted in Fig. 2 are in good agreement with the DYCOMS data. PALM simulates a well-mixed boundary layer that shows no discernible tendency of decoupling, as opposed to several members of the DYCOMS ensemble (see Stevens et al., 2005). PALM produces some overshooting at the top of the cloud layer. This can be attributed to the use of a non-monotonic advection scheme that has trouble handling

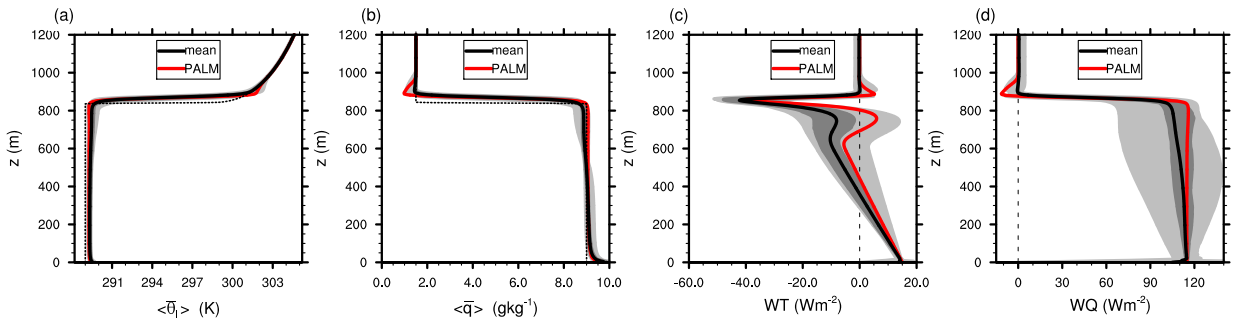

Figure 2: Vertical profiles of liquid water potential temperature $\overline{\theta}_\mathrm{l}$ (a), total water specific humidity $\overline{q}$ (b), vertical flux WT of the liquid water potential temperature (c), and vertical flux WQ of the total water specific humidity (d) for the DYCOMS case. Profiles are obtained by means of averaging over two hours of simulations. Black lines show the ensemble-mean from the DYCOMS model intercomparison study. The light grey shading shows the full range of the ensemble data, and the dark grey shading shows the interquartile range (see Stevens et al., 2005, for details). Red lines show the PALM output.

large scalar gradients. Some models from the DYCOMS ensemble reveal similar behavior with respect to the overshooting (Stevens et al., 2005).

3. SCALAR FLUX BUDGETS

Since most turbulence closure models are formulated in terms of ensemble-mean quantities, the ensemble-mean second-moment budgets should be obtained from the three-dimensional LES fields. Approximations to the ensemble-mean budgets are obtained by averaging the LES data horizontally, and the resulting profiles are then averaged over several thousand time steps. The sampling for BOMEX and DYCOMS cases is over the last three and two hours of the simulations, respectively.

In order to keep the residuals in the flux budgets as small as possible, the SGS contributions to the budgets should be accounted for. These contributions are estimated on the basis of the SGS flux-budget equations as described in e.g. Mironov (2001) and Mironov and Sullivan (2010) (but with some modifications to account for the presence of clouds). The total (resolved + sub-grid) budget of the vertical flux of scalar s is

$$\begin{aligned}
&\frac{\partial}{\partial t}\left(\left\langle \overline{u}_3''\overline{s}''\right\rangle + \left\langle \tau_{\mathrm{s}3}\right\rangle\right) = -\left(\left\langle \overline{u}_3''^2\right\rangle + \left\langle \tau_{33}\right\rangle\right)\frac{\partial\left\langle \overline{s}\right\rangle}{\partial x_3} \\
&+\frac{g}{\theta_0}\left(\left\langle \overline{s}''\overline{\theta}_\mathrm{v}''\right\rangle + \left\langle \tau_{\mathrm{vs}}\right\rangle\right) \\
&-\frac{\partial}{\partial x_3}\left[\left\langle \overline{u}_3''^2\overline{s}''\right\rangle + 2\left\langle \overline{u}_3''\tau_{\mathrm{s}3}''\right\rangle + \left\langle \overline{s}''\tau_{33}''\right\rangle + \left\langle \mathcal{T}_{3\mathrm{s}3}\right\rangle\right] \\
&-\frac{1}{\rho_0}\left(\left\langle \overline{s}''\frac{\partial\overline{p}''}{\partial x_3}\right\rangle + \left\langle \mathcal{P}_{\mathrm{s}3}\right\rangle\right).
\end{aligned} \tag{1}$$

Here, $\tau_{\mathrm{s}3} = \overline{u_3's'}$ is the vertical SGS scalar flux, and $\tau_{33} = \overline{u_3'^2}$ is the component of the SGS Reynolds-stress tensor. Both quantities are computed by the SGS model. All correlations incorporating virtual potential temperature, such as $\tau_{\mathrm{vs}} = \overline{s'\theta_\mathrm{v}'}$ and $\overline{u_3'\theta_\mathrm{v}'}$, are expressed in terms of the quasi-conservative quantities θ_l and q. The SGS virtual potential temperature-scalar covariance $\tau_{\mathrm{vs}} = \overline{s'\theta_\mathrm{v}'}$ is not computed by the SGS model. It is estimated on the basis of truncated SGS scalar-variance budgets, assuming a steady-state balance between mean-gradient production and dissipation of the SGS scalar variances. The SGS triple correlation $\mathcal{T}_{3\mathrm{s}3} = \overline{u_3'^2 s'}$ cannot be determined with our LES model and is therefore incorporated into the residual. The SGS contribution to the pressure gradient-scalar covariance, $\mathcal{P}_{\mathrm{s}3} = \overline{s'\partial p'/\partial x_3}$, is estimated on the basis of a truncated SGS scalar-flux budget, assuming a balance between mean-gradient production, buoyancy and Coriolis terms at the sub-grid scales (Mironov, 2001). Khanna (1998) and Mironov et al. (2000) showed that $\mathcal{P}_{\mathrm{s}3}$ should be accounted for in the scalar-flux budget to obtain a small residual.

The term on the left-hand side of Eq. (1) is the tendency due to nonstationarity. The terms on the right-hand side of Eq. (1) are due to the mean-gradient production/destruction G, buoyant effects B, turbulent transport Tr, and pressure gradient-scalar covariance Pr. Because of the presence of horizontally inhomogeneous radiative forcing in the DYCOMS stratocumulus-topped boundary layer case, an additional term appears in the budget of the liquid water potential temperature flux. It reads $\left\langle \overline{w}''\overline{Q}_\mathrm{r}''\right\rangle$, where $\overline{Q}_\mathrm{r}$ denotes the temperature tendency due to the radiative cooling/heating. The term $\left\langle \overline{w}''\overline{Q}_\mathrm{r}''\right\rangle$ is different

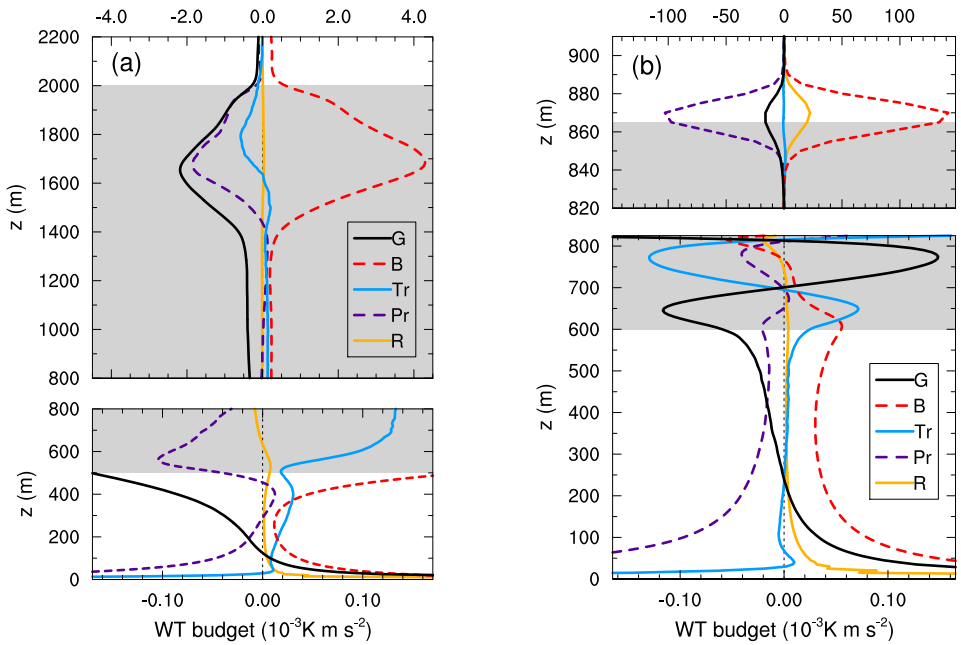

Figure 3: Budget of the vertical flux WT of the liquid water potential temperature for BOMEX (a) and DYCOMS (b). The plotted budget terms represent the effects of mean-temperature gradient G, buoyancy B, turbulent transport Tr, and pressure gradient-temperature covariance Pr, and R is the budget residual. The budget terms are averaged over three hours for BOMEX and over two hours for DYCOMS. The grey shading indicates the cloud layer. Note that a different abscissa scale is used for the upper panels.

from zero only within the cloud layer. It appears to be very small and is not shown in Fig. 3b. The time-mean of Eq. (1) is treated as an approximation to the ensemble-mean budget of the vertical scalar flux (as described in the first paragraph of the present section).

The budgets of the vertical flux of the liquid water potential temperature for BOMEX and DYCOMS are shown in Fig. 3. Since all terms in the dry mixed layer and in the lower part of the cloud layer are rather small in comparison to the upper part of the cloud layer, different scales are used for the abscissa. The mean-gradient term G changes sign where the mean-gradient changes sign. The buoyancy term B is positive throughout most of the boundary layer and acts as a source for the flux. The turbulent transport term Tr redistributes the flux in the vertical direction. It is relatively small in both cases. Another important term in the budget is the pressure gradient-scalar covariance Pr. Together with the mean-gradient term, it essentially balances the buoyant flux production. In the DYCOMS case, Fig. 3b, the pressure gradient-scalar covariance and the buoyancy term are almost mirror images as was already observed by e.g. Moeng (1986).

A comparison of Fig. 3a and Fig. 3b suggests that the main difference between the BOMEX and DYCOMS flux budgets lies in the relative importance of the mean-gradient and pressure terms near the top of the cloud layer. In the cumulus regime (Fig. 3a), G and Pr are almost equally important near the cloud top. In the stratocumulus regime (Fig. 3b), the relative importance of the pressure term is much higher. Near the cloud top, the stratocumulus temperature-flux budget is strongly dominated by the buoyancy and pressure terms. In both simulated cases, the residual R, which is defined as the sum of all budget terms, is very small over most of the boundary layer except in the near vicinity of the surface. A small residual is likely due to high resolution of our simulations and due to the inclusion of the SGS contributions into the total scalar-flux budgets. Notice, however, that in DYCOMS the residual near the cloud top is of the same order of magnitude as the mean-gradient term and is not entirely negligible. This suggests that the model has some problems with very large scalar gradients in the interfacial layer.

4. PRESSURE-SCALAR COVARIANCE

4.1 Decomposition

In second-order turbulence modeling, the standard approach to treat the pressure gradient-scalar covariance is to decompose it into contributions due to non-linear turbulence-turbulence interactions (T), mean velocity shear (S), buoyancy (B), and the Coriolis effects (C) and to model these contributions separately (e.g. Zeman, 1981). Applying this decomposition to the resolved-scale part of the covariance $\Pi_{si} = \rho_0^{-1} \langle \overline{s}'' \partial \overline{p}'' / \partial x_i \rangle$ yields

$$\Pi_{si} = \Pi_{si}^{\mathrm{T}} + \Pi_{si}^{\mathrm{S}} + \Pi_{si}^{\mathrm{B}} + \Pi_{si}^{\mathrm{C}} + \Pi_{si}^{\mathrm{SG}}. \tag{2}$$

Notice that, as different from the ensemble-mean modeling framework, an additional contribution due to the SGS Reynolds stress (SG) should be considered in the LES (see Mironov, 2001, for details). The components of Π_{si} are determined by using the corresponding contributions to the fluctuating pressure,

$$\overline{p}'' = \overline{p}''_{\mathrm{T}} + \overline{p}''_{\mathrm{S}} + \overline{p}''_{\mathrm{B}} + \overline{p}''_{\mathrm{C}} + \overline{p}''_{\mathrm{SG}}, \tag{3}$$

which in turn are determined from the following set of Poisson equations:

$$\frac{1}{\rho_0}\frac{\partial^2 \overline{p}''_{\mathrm{T}}}{\partial x_i^2} = -\frac{\partial^2}{\partial x_i \partial x_j}\left(\overline{u}_i''\overline{u}_j'' - \left\langle \overline{u}_i''\overline{u}_j'' \right\rangle\right), \tag{4}$$

$$\frac{1}{\rho_0}\frac{\partial^2 \overline{p}''_{\mathrm{S}}}{\partial x_i^2} = -2\frac{\partial \overline{u}_j''}{\partial x_i}\frac{\partial \langle \overline{u}_i \rangle}{\partial x_j}, \tag{5}$$

$$\frac{1}{\rho_0}\frac{\partial^2 \overline{p}''_{\mathrm{B}}}{\partial x_i^2} = \frac{g}{\theta_0}\frac{\partial \overline{\theta}_v''}{\partial x_3}, \tag{6}$$

$$\frac{1}{\rho_0}\frac{\partial^2 \overline{p}''_{\mathrm{C}}}{\partial x_i^2} = -\varepsilon_{ijk} f_j \frac{\partial \overline{u}_k''}{\partial x_i}, \tag{7}$$

$$\frac{1}{\rho_0}\frac{\partial^2 \overline{p}''_{\mathrm{SG}}}{\partial x_i^2} = -\frac{\partial^2}{\partial x_i \partial x_j}\overline{u_i' u_j'}''. \tag{8}$$

These Poisson equations are derived by taking the divergence of the LES momentum equation, subtracting from the resulting equation its horizontal mean (in order to obtain the equation for the deviation of pressure from its horizontal mean, $\overline{p}''$), and considering the various processes, contributing to the fluctuating pressure, separately. The pressure components obey Neumann boundary conditions at the bottom of the model domain and Dirichlet conditions at the top of the domain. This is different from Moeng and Wyngaard (1986) who used Neumann boundary conditions at the domain top. Sensitivity tests (results are not shown) indicate that the pressure components and the turbulence statistics are very little affected by the type of the upper boundary conditions. Notice that the above decomposition of the fluctuating pressure, Eq. (3), is linear so that the total fluctuating pressure should be equal (basically, to a machine precision) to the sum of its components determined from Eqs. (4)-(8). This is indeed the case in our computations.

Figure 4 shows various contributions to $\Pi_{\mathrm{q}3}$ and the sum of the contributions for BOMEX and DYCOMS. The negative of $\Pi_{\mathrm{q}3}$ is plotted as it appears in the flux-budget equation (1). In the lower part of the cloud layer and in the dry sub-cloud layer, i.e. at $z < 1400\,\mathrm{m}$ for BOMEX and at $z < 700\,\mathrm{m}$ for DYCOMS, the buoyancy B and the turbulence-turbulence T contributions are of the same order of magnitude and are roughly equally important. Near the top of the cloud layer, the buoyancy contribution B becomes increasingly important and dominates the total pressure gradient-humidity covariance. The shear contribution S is only significant near the surface in both simulated cases, whereas the Coriolis contribution (C, not shown) is two orders of magnitude smaller than other contributions and can safely be neglected. The contribution SG due to SGS stress is small, confirming the fidelity of our LES results. The analysis of the covariance of the vertical pressure gradient and the liquid water potential temperature, $\Pi_{\theta 3}$, yields similar results as for the relative importance of the various contributions (not shown). For both q and θ_{l}, the pressure gradient-scalar covariance is dominated by buoyancy and turbulence-turbulence effects.

4.2 Testing parameterizations of the pressure-scalar covariance against LES data

As the contributions to the pressure gradient-scalar covariance due to buoyancy B and turbulence-turbulence interactions T are the most important ones for our cloudy boundary-layer cases (Fig. 4), some commonly used parameterizations for these contributions are tested against LES data.

4.2.1 Buoyancy contribution to Π_{si}

A simple parameterization for the buoyancy contribution Π_{si}^{B} to the pressure gradient-scalar covariance that is commonly used in applications reads

$$\Pi_{si}^{\mathrm{B}} = c_{\mathrm{B}} \frac{g}{\theta_0}\delta_{i3}\left(\left\langle \overline{s}''\overline{\theta}_{\mathrm{v}}'' \right\rangle + \langle \tau_{\mathrm{vs}} \rangle\right). \tag{9}$$

Note that Eq. (9) is linear in the second-order moments. It sets Π_{si}^{B} proportional to the buoyancy term in the scalar flux budget Eq. (1). Therefore, it simply compensates a part of the buoyancy production of the scalar flux. A theoretical value of dimensionless constant c_{B} that stems from isotropic tensor modeling (see e.g. Lumely, 1978; Zeman, 1981; Hanjalić and Launder, 2011) is $1/3$. Moeng and Wyngaard (1986) found, however, that a value of $c_{\mathrm{B}} = 0.5$ is more consistent with the data from LES of slightly sheared convective boundary

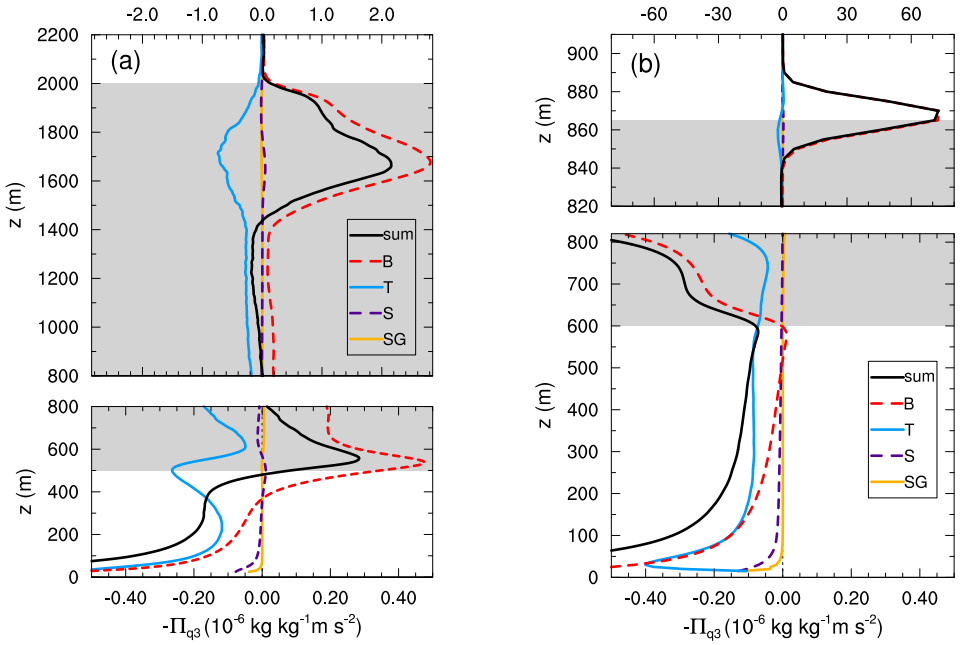

Figure 4: Contributions to the covariance of the vertical pressure gradient and the total water specific humidity, Π_{q3}, due to buoyancy B, turbulence-turbulence interactions T, mean velocity shear S, and SGS stress SG for BOMEX (a) and DYCOMS (b). Black solid lines show the sum of the various contributions. Notice that the turbulence-turbulence contribution does not include the SGS part $\mathcal{P}_{q3} = \overline{q' \partial p'/\partial x_3}$ (see Eq. (1) and section 4.2.2). The averaging time is three hours for BOMEX and two hours for DYCOMS.

layer.

Figure 5 compares Π^{B}_{q3} from the LES data with its parameterization through Eq. (9). Apart from the estimates of $c_B = 1/3$ and $c_B = 0.5$, we have used the best-fit value of c_B obtained with the least-squares method. The fitting is applied over the middle part of the boundary layer, at $100\,\mathrm{m} < z < 2000\,\mathrm{m}$ for BOMEX and at $100\,\mathrm{m} < z < 800\,\mathrm{m}$ for DYCOMS, excluding the near-surface layer and the interfacial layer. For both cumulus and stratocumulus boundary layers, the LES data and the parameterization agree quite well. The shape of the Π^{B}_{q3} profile is captured well by Eq. (9). There is some underestimation of the LES data, particularly near the cloud top. The best-fit values of c_B are 0.51 and 0.49 for BOMEX and DYCOMS, respectively, that is the same as $c_B = 0.5$ found by Moeng and Wyngaard (1986). A consideration of the buoyancy contribution to the vertical pressure gradient-temperature covariance, $\Pi^{B}_{\theta 3}$, also indicates a good performance of Eq. (9). The best-fit estimates of c_B are found to be 0.46 and 0.45 for BOMEX and DYCOMS, respectively. Our analysis of Π^{B}_{s3} suggests that a linear parameterization (9) with $c_B = 0.5$ can be recommended for use in cloudy boundary layer modeling.

It is worthy of note, however, that Eq. (9) yields a non-zero value for the vertical component Π^{B}_{s3} of Π^{B}_{si} (aligned with the vector of gravity). A linear parameterization (9) is unable to account for the horizontal components ($i = 1$ or $i = 2$) of Π^{B}_{si}. This is at variance with our LES data (not shown) indicating that Π^{B}_{s1} and Π^{B}_{s2} are important contributions to the pressure gradient-scalar covariances (along with the turbulence-turbulence contributions) and should be taken into account. To this end, more sophisticated models of Π^{B}_{si} are required, e.g. a nonlinear two-component-limit model of Craft et al. (1996).

4.2.2 *Turbulence-turbulence contribution to* Π_{si}

A Rotta-type (Rotta, 1951) relaxation (return-to-isotropy) parameterization is commonly used for the turbulence-turbulence contribution to the pressure gradient-scalar covariance. It reads (e.g. Zeman, 1981)

$$\Pi^{T}_{si} = \frac{c_T}{\tau}\left(\left\langle \overline{u}_i'' \overline{s}'' \right\rangle\right) + \left\langle \tau_{si} \right\rangle\right), \qquad (10)$$

where c_T is a dimensionless constant, and τ is a relaxation "return-to-isotropy" time-scale for a scalar quantity s. The time-scale τ is often set proportional to the TKE dissipation time-scale $\tau_\varepsilon = TKE/\varepsilon$, where ε is the TKE dissipation rate. According to Zeman (1981), the values

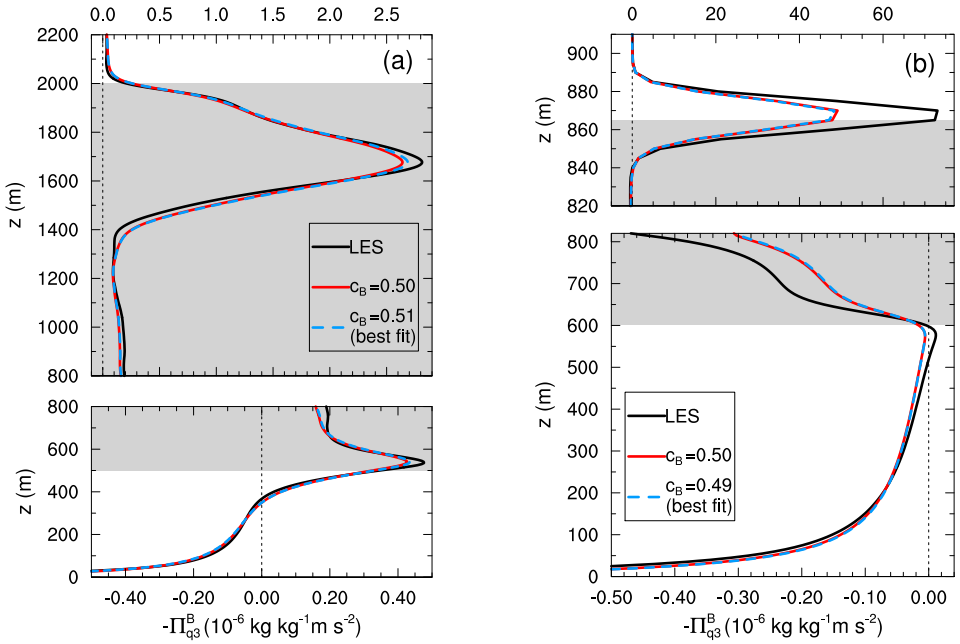

Figure 5: Buoyancy contribution of the covariance of the vertical pressure gradient and the total water specific humidity, $\Pi^{\mathrm{B}}_{\mathrm{q}3}$, for BOMEX (a) and DYCOMS (b). Black lines show $\Pi^{\mathrm{B}}_{\mathrm{q}3}$ from the LES data. Red lines show the linear parameterization, Eq. (9), with $c_{\mathrm{B}} = 0.5$, and blue lines show the linear parameterization with the best-fit value of c_{B} based on a least-squares method. The averaging time is three hours for BOMEX and two hours for DYCOMS.

of c_{T} lie between 3 and 5. For dry convective boundary layers, an estimate of $c_{\mathrm{T}} = 3.0$ was obtained on the basis of LES data (Mironov, 2001).

In Fig. 6, the turbulence-turbulence contribution $\Pi^{\mathrm{T}}_{\theta 3}$ from LES is compared with its parameterization through Eq. (10). The TKE $\langle e \rangle = \frac{1}{2}\left\langle \overline{u}_i'^2 + \overline{u_i'^2} \right\rangle$ is estimated with due regard for the SGS contribution, and the TKE dissipation rate $\langle \varepsilon \rangle$ is estimated as a residual of the total (resolved + sub-grid) TKE budget. Following Mironov (2001), the SGS contribution to the pressure gradient-scalar covariance, $\mathcal{P}_{s3}$ (see section 3.), is added to the turbulence-turbulence part of the resolved pressure gradient-scalar covariance. In the remainder of this section, Π^{T}_{si} denotes the sum of the resolved and SGS contributions.

The Rotta-type parameterization of $\Pi^{\mathrm{T}}_{\theta 3}$ agrees satisfactorily with the LES data over most of the boundary layer except near the cloud top, where Eq. (10) underestimates data. The shape of the $\Pi^{\mathrm{T}}_{\theta 3}$ profile is not reproduced accurately enough. For example, the local maximum at cloud base in the BOMEX case and the maxima near the cloud top in both cases are not caught. The best-fit values of c_{T} (obtained with the least-squares method) proved to be 4.16 and 3.19 for BOMEX and DYCOMS, respectively. These values lie within the range $3 \leq c_{\mathrm{T}} \leq 5$ reported by Zeman (1981). For the horizontal components of the pressure gradient-temperature covariance (not shown), the best-fit estimates of c_{T} appeared to vary quite significantly. For $\Pi^{\mathrm{T}}_{\theta 1}$, the best-fit values of c_{T} are 1.69 for BOMEX and 3.83 for DYCOMS, and for $\Pi^{\mathrm{T}}_{\theta 2}$, the values are 1.51 for BOMEX and 2.34 for DYCOMS. For Π^{T}_{qi}, similar results are obtained, indicating that no universal best-fit estimate of the dimensionless constant c_{T} can be found that is valid for both types of cloudy boundary layers and for all spatial directions. This suggests that the Rotta-type parameterization of the turbulence-turbulence contribution to the pressure-gradient scalar covariance is somewhat oversimplified. A more elaborate parameterization will hopefully do a better job.

5. CONCLUSIONS

Large-eddy simulations of shallow cumulus-topped and stratocumulus-topped boundary layer flows are used to compute various statistical moments of fluctuating fields of velocity and scalar quantities (liquid water potential temperature and total water specific humidity) and to estimate terms in the budget equations for the scalar fluxes. In order to close the flux budgets to a good order, SGS

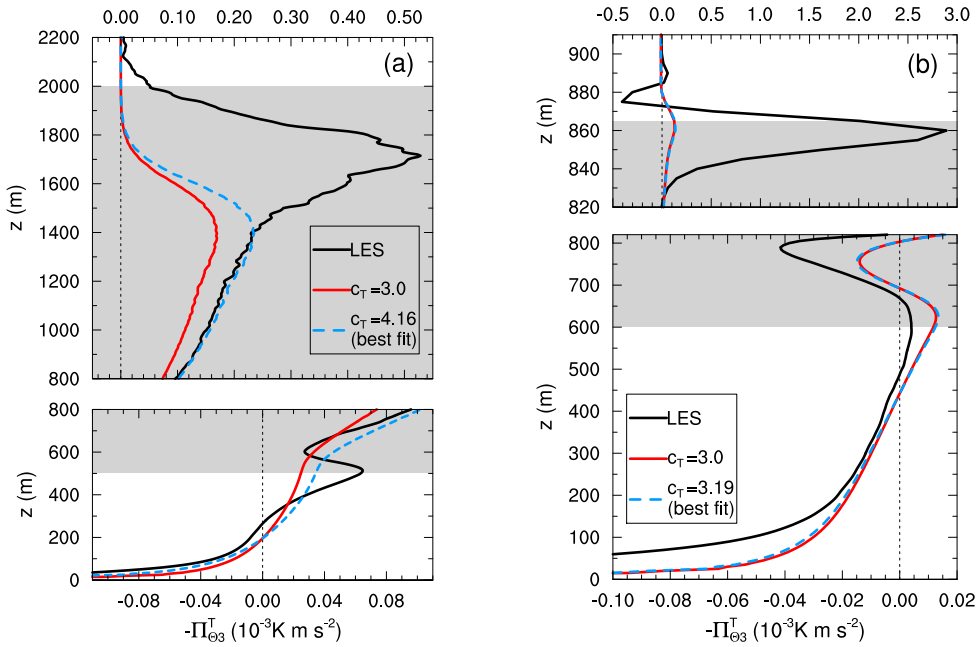

Figure 6: Turbulence-turbulence contribution of the covariance of the vertical pressure gradient and the liquid water potential temperature, $\Pi^T_{\theta 3}$ for BOMEX (a) and DYCOMS (b). Black lines show $\Pi^T_{\theta 3}$ from the LES data. Red lines show the Rotta-type return-to-isotropy parameterization, Eq. (10), with $c_T = 3.0$, and blue lines show the return-to-isotropy parameterization but with the best-fit value for c_T based on a least-squares method. The averaging time is three hours for BOMEX and two hours for DYCOMS.

contributions to various budget terms are taken into account. The pressure scrambling terms in the flux budgets (i.e. the pressure gradient-scalar covariances) are decomposed into contributions due to turbulence-turbulence interactions, buoyancy, mean velocity shear, and Coriolis effects, and the performance of some commonly used parameterizations for the pressure terms is tested against LES data.

In cloudy boundary layers, the scalar-flux budgets are found to be dominated by the buoyancy, the mean-scalar-gradient, and the pressure-scrambling terms. The pressure gradient-scalar covariances are mainly determined by the buoyancy and the turbulence-turbulence contributions, whereas the shear contribution is only significant near the surface. A simple linear parameterization for the buoyancy contribution to the pressure gradient-scalar covariance shows a good performance. The Rotta-type relaxation parameterization of the turbulence-turbulence contribution performs less satisfactorily. It strongly underestimates LES data near the cloud top and has some trouble reproducing the shape of the vertical profile of the turbulence-turbulence contributions. To improve the quality of cloudy boundary layer turbulence modeling, more sophisticated parameterizations are required. For example, a two-component-limit formulation of Craft et al. (1996) showed promising results for dry convective boundary layers (Mironov, 2001). Comprehensive testing for cloudy boundary layers is still to be performed.

Acknowledgments. This study was supported by the *Extramurale Forschung* Program of the German Weather Service and by the European Commission through the COST Action ES0905. All simulations were performed on the SGI Altix ICE of the *The North-German Supercomputing Alliance* (HRLN), Hannover and Berlin, Germany.

REFERENCES

Andrén, A. and C.-H. Moeng, 1993: Single-point closure in a neutrally stratified boundary layer, *J. Atmos. Sci.*, **50**, 3366–3379.

Brown, A. R., 1999: Large-eddy simulation and parameterization of the effects of shear on shallow cumulus convection, *Boundary-Layer Meteorol*, **91**, 65–80.

Chlond, A. and A. Wolkau, 2000: Large-eddy simulation of a nocturnal stratocumulus-topped marine atmospheric boundary layer: an uncertainty analysis, *Boundary-Layer Meteorol*, **95**, 31–55.

Craft, T. J., N. Z. Ince, and B. E. Launder, 1996: Recent developments in second-moment closure for buoyancy affected flows, *Dyn. Atmos. Oceans*, **23**, 99–114.

Cuijpers, J. W. M. and P. G. Duynkerke, 1993: Large eddy simulation of trade wind cumulus clouds, *J. Atmos. Sci.*, **50**, 3894–3908.

Cuijpers, J. W. M., P. G. Duynkerke, and F. T. M. Nieuwstadt, 1996: Analyses of variance and flux budgets in cumulus-topped boundary layers, *Atmos. Res.*, **40**, 307–337.

de Roode, S. R. and C. S. Bretherton, 2003: Mass-flux budgets of shallow cumulus clouds, *J. Atmos. Sci.*, **60**, 137–151.

Deardorff, J. W., 1980: Stratocumulus-capped mixed layers derived from a three-dimensional model, *Boundary-Layer Meteorol.*, **18**, 495–527.

Hanjalić, K. and B. Launder, 2011: *Modelling Turbulence in Engineering and the Environment - Second-Moment Routes to Closures*, Cambridge University Press, 379 pp.

Khanna, S., 1998: Comparison of Kansas data with high-resolution large-eddy simulation fields, *Boundary-Layer Meteorol.*, **88**, 121–144.

Lumely, J. L., 1978: Computational modeling of turbulent flows, *Adv. Appl. Mech.*, **18**, 123–176.

Mironov, D. V., 2001: Pressure-potential temperatur covariance in convection with rotation, *Quart. J. Roy. Meteor. Soc.*, **127**, 89–110.

—, 2009: Turbulence in the lower troposphere: second-order closure and mass-flux modelling frameworks, *Lect. Notes Phys.*, **756**, 161–221.

Mironov, D. V., V. M. Gryanik, C.-H. Moeng, D. J. Olbers, and T. H. Warncke, 2000: Vertical turbulence structure and second-moment budgets in convection with rotation: A large-eddy simulation study, *Quart. J. Roy. Meteor. Soc.*, **126**, 477–515.

Mironov, D. V. and P. P. Sullivan, 2010: Effect of horizontal surface temperature heterogeneity on turbulent mixing in the stably stratified atmospheric boundary layer, in *19th Amer. Meteorol. Soc. Symp. on Boundary Layers and Turbulence*, pp. 10, paper 6.3, Keystone, USA.

Moeng, C.-H., 1986: Large-eddy simulation of a stratus topped boundary layer. Part I: structure und budgets, *J. Atmos. Sci.*, **43**, 2880–2900.

Moeng, C.-H. and J. C. Wyngaard, 1986: An analyis of closures for pressure-scalar convariances in the convective boundary layer, *J. Atmos. Sci.*, **43**, 2499–2513.

NCL, 2012: The NCAR Command Language (Version 6.0.0) [Software]. Boulder, Colorado: UCAR/NCAR/CISL/VETS. http://dx.doi.org/10.5065/D6WD3XH5.

Neggers, R. A. J., 2009: A dual mass flux framework for boundary layer convection. Part II: clouds, *J. Atmos. Sci.*, **66**, 1489–1506.

Raasch, S. and M. Schröter, 2001: PALM – A large-eddy simulation model performing on massively parallel computers, *Meteor. Z.*, **10**, 363–372.

Riechelmann, T., Y. Noh, and S. Raasch, 2012: A new method for large-eddy simulations of clouds with Lagrangian droplets including the effects of turbulent collision, *New J. Phys.*, **14**, 27.

Rotta, J. C., 1951: Statistische Theorie nichthomogener Turbulenz. 1., *Zs. Phys.*, **129**, 547–572.

Schumann, U., 1975: Subgrid scale model for finite difference simulations of turbulent flows in plane channels and annuli, *J. Comput. Sci.*, **18**, 376–404.

Siebesma, A. P., C. S. Bretherton, A. Brown, A. Chlond, J. Cuxart, P. G. Duynkerke, H. Jiang, M. Khairoutdinov, D. Lewellen, C.-H. Moeng, E. Sanchez, B. Stevens, and D. E. Stevens, 2003: A large eddy simulation intercomparison study of shallow cumulus convection, *J. Atmos. Sci.*, **60**, 1201–1219.

Stevens, B., C.-H. Moeng, A. S. Ackermann, C. S. Bretherton, A. Chlond, S. de Roode, J. Edwards, J.-C. Golaz, H. Jiang, A. Khairoutdinov, M. P. Kirkpatrick, D. C. Lewellen, A. Lock, F. Mller, D. E. Stevens, E. Whelan, and P. Zhu, 2005: Evaluation of large-eddy simulations via observations of nocturnal marine stratocumulus, *J. Atmos. Sci.*, **133**, 1443–1462.

Wicker, L. J. and W. S. Skamarock, 2002: Time-splitting methods for elastic models using forward time schemes, *J. Atmos. Sci.*, **130**, 2088–2097.

Wilczak, J. M. and A. J. Bedard, 2004: A new turbulence microbarometer and its evaluation using the budget of horizontal heat flux, *J. Atmos. Oceanic Technol.*, **21**, 1170–1181.

Zeman, O., 1981: Progress in the modelling of planetary boundary layers, *Ann. Rev. Fluid Mech.*, **13**, 253–272.